The Journal of Physical Chemistry Letters

Letter

Cite This: J. Phys. Chem. Lett. 2018, 9, 7130−7136

pubs.acs.org/JPCL

Geometry Distortion and Small Polaron Binding Energy Changes with Ionic Substitution in Halide Perovskites

Amanda J. Neukirch,[*,†] Iwnetim I. Abate,[∥,∇] Liujiang Zhou,[†] Wanyi Nie,[‡] Hsinhan Tsai,[‡] Laurent Pedesseau,[#] Jacky Even,[#] Jared J. Crochet,[§] Aditya D. Mohite,[○] Claudine Katan,[⊥] and Sergei Tretiak[†]

[†]Theoretical Physics and Chemistry of Materials, Los Alamos National Laboratory, Los Alamos, New Mexico 87545, United States

[∥]Department of Materials Science and Engineering, Stanford University, Stanford, California 94305, United States

[∇]Stanford Institute for Materials and Energy Sciences, SLAC National Accelerator Laboratory, Menlo Park, California 94025, United States

[‡]Materials Physics and Application, Los Alamos National Laboratory, Los Alamos, New Mexico 87545, United States

[§]Physical Chemistry and Applied Spectroscopy Division, Los Alamos National Laboratory, Los Alamos, New Mexico 87545, United States

[#]Univ Rennes, INSA Rennes, CNRS, Institut FOTON - UMR 6082, F-35000 Rennes, France

[○]Department of Chemical and Biomolecular Engineering, Rice University, Houston, Texas 77006, United States

[⊥]Univ Rennes, ENSCR, INSA Rennes, CNRS, ISCR - UMR 6226, F-35000 Rennes, France

Supporting Information

ABSTRACT: Halide perovskites have demonstrated remarkable performance in optoelectronic applications. Despite extraordinary progress, questions remain about device stability. We report an in-depth computational study of small polaron formation, electronic structure, charge density, and reorganization energies of several experimentally relevant halide perovskites using isolated clusters. Local lattice symmetry, electronic structure, and electron−phonon coupling are interrelated in polaron formation in these materials. To illustrate this, first-principles calculations are performed on (MA/Cs/FA)Pb(I/Br)$_3$ and MASnI$_3$. Across the materials studied, electron small polaron formation is manifested by Jahn−Teller-like distortions in the central octahedron, with apical PbI bonds expanding significantly more than the equatorial bonds. In contrast, hole polarons cause the central octahedron to uniformly contract. This difference in manifestation of electron and hole polaron formation can be a tool to determine what is taking place in individual systems to systematically control performance. Other trends as the anion and cations are changed are established for optimization in specific optoelectronic applications.

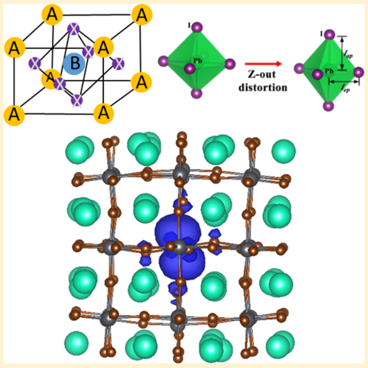

Solution-processed halide perovskites (HPs) are promising candidates for a diverse range of applications, including photovoltaics, light-emitting diodes,[1,2] hydrogen generation,[3] X-ray and gamma-ray detection,[4,5] spintronics,[6] and sensor applications.[7] They combine low solution-processing costs with composition of earth abundant materials. Further development of perovskite materials requires a fundamental understanding of structure−property relationships in order to control emergent optoelectronic properties through materials design.

We recently demonstrated the reduction of photocurrent in crystalline large grain perovskite solar cells of MAPbI$_3$ under constant solar illumination.[8] The efficiency recovers to its original value after less than 1 min in the dark. Our previous studies attributed the photodegradation to light-activated metastable trap states of atomistic origin.[8,9] Our experimental and theoretical characterizations in those previous studies suggested that localized charged states strongly couple to local structural lattice distortions and methylammonium (MA) quasi-static configurations. The presence of a charge initiates lattice distortions that then stabilize the charge in a spatially confined area. These seed the formation of macroscopic charged domains, preventing efficient charge extraction.

Since this initial prediction of small polaron formation in HPs, several groups using spectroscopic techniques and ab initio calculations have found evidence of polaron formation in MAPbI$_3$,[10−12] MAPbBr$_3$ (bulk[13] and nanoparticle[14]), MAPb(I$_x$Br$_{1-x}$)$_3$,[15] CsPbBr$_3$,[16] 2D APbCl$_4$ and MAPbBr$_4$,[17,18] and wide-bandgap defect HPs A$_3$M$_2$I$_9$ (A = Cs, Rb; M = Bi, Sb).[19,20] Polaronic species are reported to be either holes[11,16]

Received: November 2, 2018
Accepted: December 7, 2018
Published: December 7, 2018

DOI: 10.1021/acs.jpclett.8b03343
J. Phys. Chem. Lett. 2018, 9, 7130−7136

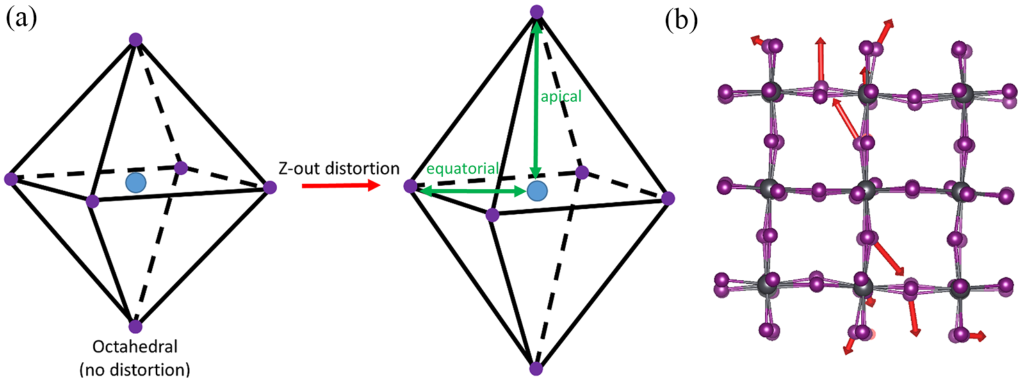

Figure 1. (a) Schematic of Jahn−Teller distortion. (b) Optimized neutral PbI_3 framework of the $CsPbI_3$ cluster with arrows on the atoms that move the most and point in the direction of the same atoms within the optimized charged cluster (atomic displacements are scaled by a factor of 3 for clarity).

or electrons,[14] while some studies suggest that the polaron formation is facilitated by defects or interface disorder.[10,11] A recent experimental−theoretical work quantified lattice displacements when photoexcited excitons evolve into a polaronic state.[12] There is experimental evidence that hole polaron formation is the initial stage of iodide vacancy.[21] Polaron formation could be responsible for halide phase separation, specifically localized strain induced by photoexcited charge interacts with the soft ionic lattices to promote halide phase separation.[15] In addition, photoinduced strain in $MAPbBr_3$ is said to cause large blue shifts to its Raman spectra that indicate significant structural deformations; this photostriction is stable for 30 days.[13] A recent contribution found that the formation of small polarons required the copresence of MA, Sn, and Br.[22] Thus, further understanding of small polaron formation in various metal halide perovskites is highly necessary to provide the foundations of engineering applied to optoelectronic devices

In this Letter, we report density functional theory (DFT) simulations of small polaron binding energy as a function of chemical composition in a variety of halide perovskites. We show first that replacing MA with FA lowers the polaron binding energy below that of $MAPbI_3$. Indeed, the formation of small polarons in $MAPbI_3$ was initially traced to MA rotation *and* volumetric lattice strain.[9] This interpretation was consistent with lower polaron binding energies in $CsPbI_3$ for both electrons and holes and led to the hypothesis that $FAPbI_3$ would be the best pure material to alleviate the photodegradation.[11] Further systematic studies are performed by substituting Pb with Sn in $MAPbI_3$ and I with Br in $MAPbI_3$, $CsPbI_3$, and $FAPbI_3$. Finally, conclusions are drawn on the influence of lattice symmetry, electronic structure, and electron−phonon coupling on the formation of small polarons in HPs. It is found that for electrons the polaron binding energy gets smaller as the A-site cation is changed from MA to Cs to FA. Less intuitive is that Br substitution tends to create a larger electron polaron binding energy and a smaller hole polaron binding energy. $MASnI_3$ has smaller polaron binding energies for electrons and holes compared to $MAPbI_3$. Structurally, formation of electron polarons is universally concomitant to the central Pb-halide bond expansion by about 25% in one direction, forming a Jahn−Teller distortion. It should be noted that local central symmetry breaking such as this should lead to larger Rashba-like splitting in hybrid perosvkites.[23] Hole polarons see the central Pb-halide bonds contract uniformly in all directions. The observed difference in structural changes of the lattice between hole and electron polarons can be used to identify which species are dominant in a given experimental system.

We briefly note that because of the size of the systems, use of hybrid functional, and intentional use of local basis functions, spin−orbit coupling (SOC) could not be taken into account for these calculations. This does add a few caveats to our results. The electron reorganization and polaron binding energies will be overestimated because of the lack of inclusion of SOC. Previously, we have also observed that because our calculations do not have SOC to correctly break the degeneracy at the bottom of the conduction band, the Jahn−Teller distortions and displacements we calculate are larger than those observed in experiment.[12] In spite of these caveats, general trends across the materials series are predicted correctly, particularly for the Pb perovskites. Comparisons between Sn and Pb systems are a little bit trickier as the SOC contribution in Sn materials is smaller, and therefore, those results should be less overestimated.[24] Other attempts to reduce the computational complexity in perovskite systems including SOC were performed by replacing hybrid functionals with DFT+U[25] or using the Tran−Blaha modified Becke−Johnson exchange potential approximation.[26] The rest of the computational details are presented at the end of the Letter and in the Supporting Information. Below we briefly highlight some important facts about each material studied as well as the reference bulk geometry used.

$MAPbI_3$: Most ubiquitous perovskite material. This material had rapid success in the solar cell community and is still in use in perovskite alloys with 23.3% efficiency currently.[27] However, it has been shown that the pure material is unstable under continuous exposure to light,[8] and small polaron formation was proposed as one of the possible mechanisms in addition to iodide vacancy migration.[9] We started from space group $Pm\bar{3}m$ with cubic lattice parameters calculated from the low-temperature tetragonal supercell derived from variable-temperature powder X-ray diffraction experiments.[28]

$CsPbI_3$: Simplified version of $MAPbI_3$, important for state-of-the-art quantum dot-based solar cells.[27] Our reference bulk structure was a cubic perovskite structure with space group $Pm\bar{3}m$ and a lattice parameter derived from variable-temperature powder X-ray diffraction.[29]

$FAPbI_3$: $FAPbI_3$ is the main component of state of the art alloys for solar cell applications and of interest because it is the most likely pure material to reduce polaron formation. Our reference bulk structure was from the *Imm*2 space group determined from X-ray diffraction experiments.[30]

$MAPbBr_3$: The polaron concept has been used to explain the I/Br phase separation[31−34] in $MAPbBr_3$ (bulk[13] and nanoparticle[14]), $MAPb(I_xBr_{1-x})_3$,[15] and $MAPbBr_4$,[17,18] Here we start from the refined neutron powder diffraction *Pnma* structure.[35,36]

$FAPbBr_3$: Our reference bulk structure was from the *Imm*2 space group, similar to $FAPbI_3$, but using lattice parameters that take into account Br instead of I.

$CsPbBr_3$: Our reference bulk structure was a cubic perovskite structure with space group $Pm\bar{3}m$ and using a lattice parameter that was derived to give the same volume per unit cell as the orthorhombic *Pnma* $CsPbBr_3$.[37]

$MASnI_3$: One goal of the perovskite community is to remove Pb from the formula, and replacing Pb with nontoxic Sn is the simplest way to achieve that goal. Our reference bulk structure was the experimentally determined tetragonal structure with space group *P*4*mm*.[38]

One important aspect of carrier self-trapping is symmetry breaking, which may show itself in the activation of normally forbidden infrared modes.[39,40] Electron coupling with acoustic or polar optical phonons leads to different polaronic species in semiconductor lattices with well-defined point group symmetries.[9] Empirical Hamiltonians, like Holstein's,[40] are built to introduce a nonlinearity into Schrödinger's equation and provoke a bifurcation. A purely small polaron scenario related to totally symmetric local strain was presented in our previous contribution.[9] The importance of electron polarons for both $MAPbI_3$ and $CsPbI_3$ through Jahn−Teller (JT) distortions[41,42] is yet undiscussed (Figure 1). A distortion is typically observed among octahedral complexes where the two apical bonds are longer than the equatorial bonds. The JT distortion is intimately linked to electronic degrees of freedom because, traditionally, it manifests to remove an electronic degeneracy, opening a band gap and favoring a particular electronic state, all of which are quite common in perovskite materials.[43,44]

In Ge- or Cl-based HPs, these polar and anisotropic distortions are commonly spread over the entire lattice,[24] but in this work we show that it plays an important role at the local scale for polaronic states in all the HPs. To do this, we compare bond lengths, tilt angles, and energies of clusters that are optimized when neutral to clusters that are optimized when charged. The hole polaron bond lengths (in the central octahedron) universally shrink by 5% in all directions (Table 1). The fact that all systems exhibit a negative and isotropic effect for holes and positive and anisotropic effects for electrons suggests that while bond length variations are important for polaron formation, the two types of carriers must be discussed separately. Indeed, for the electron polaron in all materials studied here, the bond lengths of the four equatorial metal/halide bonds in the central octahedral remain almost unchanged compared to the neutrally optimized system, and the two apical bond lengths undergo a sizable increase, by about 25% (Table 1). Again the contribution of the phonon mode associated with Jahn−Teller distortions using this method appears to be overestimated in comparison to experiment.[12] This is likely due to the exclusion of SOC in the present study. Therefore, there is a spurious true degeneracy that is broken with the addition of the charge, while in real systems SOC already lifts this conduction band degeneracy; thus, the observed anisotropic effect should not be as strong. However, the observed variations of local octahedra geometries for electrons and holes is a general and genuine trend (Figure 1b).

Table 1. Change in PbI Equatorial and Apical Bond Lengths (Figure 1) of the Central Octahedron

	change in Pb−I bond length (%)		
	electron		hole
	equatorial	apical	equatorial and apical
$MAPbI_3$	2	25	−5
$CsPbI_3$	2	32	−5
$FAPbI_3$	−2	23	−6
$MAPbBr_3$	2	21	−5
$CsPbBr_3$	2	37	−6
$FAPbBr_3$	2	27	−6
$MASnI_3$	2	27	−5

The in-plane octahedral tilting of the central octahedron between the neutral and charged systems (Figure 2a) depends strongly on the constituent ions. Besides bond length variations, it is an efficient way to locally relax the lattice strain.[45] Such angular variations have been linked to the evolution of the electronic band gap with respect to structural deformation of the perovskite.[46−49] Across all systems studied, MA-based compounds exhibit the largest changes of in-plane tilt angles (Table 2). Moreover, electron localization is more likely to induce a large in-plane tilt angle than hole localization.

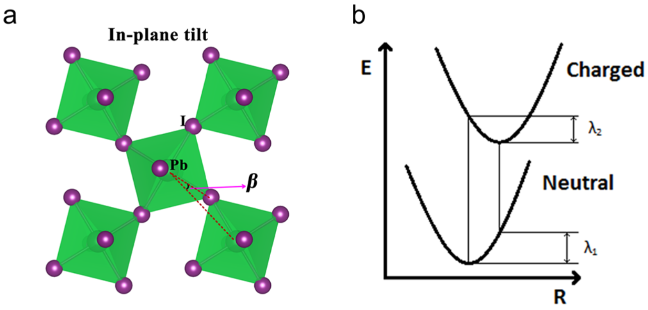

Figure 2. Definition of the (a) in-plane tilt angle β and (b) internal reorganization energies of the small polaron: polaron binding energy λ_2 and change in energies of the neutral species λ_1.

To further explore the polaronic picture, we switch from the characterization of the local lattice distortions by both bond elongations and tilt angles to the modifications of the electronic properties. In order to quantify the polaron binding

Table 2. Average Change of In-Plane Tilt Angle between the Optimized Neutral System and the Optimized Charged System

	change of in-plane tilt angle (deg)	
	electron	hole
$MAPbI_3$	5.3	0.3
$CsPbI_3$	0.5	2.1
$FAPbI_3$	0.3	1.0
$MAPbBr_3$	5.7	−0.1
$CsPbBr_3$	2.7	1.1
$FAPbBr_3$	1.1	1.3
$MASnI_3$	6.5	0.3

energy, we calculate the two relaxation energies, the sum of which is the reorganization energy, further described in the Supporting Information, in a standard Marcus theory describing electron transfer (Figure 2b).[50] The internal reorganization energy essentially quantifies variation of electronic energy due to the geometry changes when an electron is added or removed from the cluster.[51]

It is found that for electrons in iodide compounds, the polaron binding energy, λ_2, gets smaller as the A-site cation is changed from MA to Cs to FA. Going from I to Br typically reduces the binding energy for holes. $MAPbBr_3$ has a substantially lower polaron binding energy for electrons compared to $MAPbI_3$, but going from I to Br with Cs or FA as the cation causes the polaron binding energy to get larger. Bromide compounds have a larger λ_1 than corresponding iodide compounds. This is consistent with the experimental observation of the enhanced softness of the latter compounds.[52] Interestingly, it has been shown that Br-based perovskites have stronger electron−phonon coupling compared to I perovskites.[53] We find that $MASnI_3$ has smaller polaron binding energies for electrons and holes compared to $MAPbI_3$; however, it is expected to be less overestimated for electrons because Sn has smaller contributions from SOC.[24]

Changes in polaron binding strength, λ_2, correspond to changes in polaron size. Figure 3 (top row) shows the spin density of the electron polaron created in the $CsPbI_3$ system (λ_2 = 918 meV) is more localized than that of the $FAPbI_3$ system (λ_2 = 723 meV) for the same isosurface value. The same trend holds when comparing $CsPbBr_3$ (λ_2 = 1270 meV) to $FAPbBr_3$ (λ_2 = 1064 meV) (Figure S1). Figure 3 (bottom row) displays that the hole polaron for the $MAPbI_3$ system (λ_2 = 578 meV) is more localized than the hole polaron for $MAPbBr_3$ (λ_2 = 275 meV).

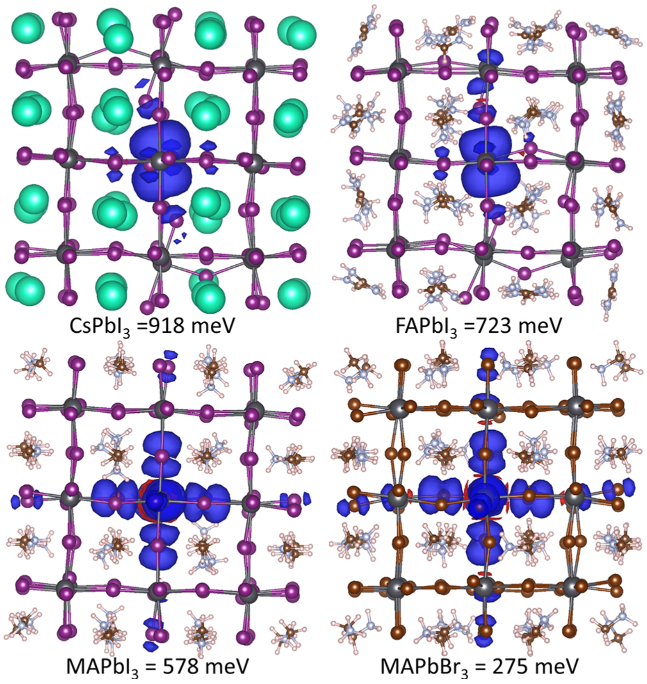

Figure 3. Top row: Spin density comparing the electron polaron in the $CsPbI_3$ system (left) and $FAPbI_3$ system (right). Bottom row: Spin density comparing the hole polaron in the $MAPbI_3$ system (left) and $MAPbBr_3$ system (right). (Isosurface of 0.0002 a_0^{-3}).

A general trend in electron and hole small polaron formation is that the induced local volume variations are opposite. This trend might be useful for experimental detection of polaron type. With a wide variety of experimental evidence pointing to everything from large polarons,[54] or only electron polarons,[14] or only hole polarons,[11,16] there is the possibility that what minority carriers populate a given system or device depends on a number of factors, including the crystal quality, surfaces, contacts, and interfaces.[10,22] Thus, a particular system may be more prone to electron or hole small polaron formation, and as we see from the computed data (Table 3), the materials that minimize polaron binding energy are different for electrons and holes. We believe the results presented in this Letter demonstrate that polaronic effects in iodide compounds will decrease when going from MA to Cs to FA. However, there are a couple of areas that require more consideration and discussion when putting the results presented in this Letter into context, namely, material elasticity and dimensionality.[45,52]

Table 3. Reorganization Energies (in meV) for Charged Clusters Computed Using the CAM-B3LYP Functional

	electron			hole		
	λ_1	λ_2	λ	λ_1	λ_2	λ
$MAPbI_3$	510	1377	1887	528	578	1106
$CsPbI_3$	724	918	1642	365	274	639
$FAPbI_3$	536	723	1259	310	533	816
$MAPbBr_3$	1230	816	2046	566	275	841
$CsPbBr_3$	857	1270	2127	486	342	828
$FAPbBr_3$	719	1064	1783	379	433	812
$MASnI_3$	519	1059	1578	268	460	730

This study provides only a glimpse of the depth of the potential energy surfaces. Our simulations give no information about the stiffness of the local potentials or the time scale for formation of lattice distortions. It is likely that while a system has the potential to form a very deep polaron, the time scale to do so is so slow that the carriers are extracted before polaron formation. It is important to note that charge carriers moving in hybrid perovskite compounds experience an extremely perturbed electrostatic landscape due to stochastic structural fluctuations of the organic and inorganic components and other sources of lattice softness.[55] Furthermore, elasticity characterizes the ability of a lattice to undergo long-range strain. It has been established that Br-based systems have indeed a higher bulk modulus than I-based perovskites and are therefore stiffer and less prone to long-range distortions.[52,56] It should be noted that the present study probes only local distortions; the bond lengths and tilting within the central octahedron of Br-based system involves more atomic displacement compared to the I-based system. It is thus likely that our simulation is capturing only the short-range distortions produced by the small polarons but not properly capturing long-range distortions owing to the small size of the computed clusters. The missing long-range part of the lattice distortions around the small polarons may reduce the predicted energetic differences between Br and I materials as well as the comparative localization of electrons and holes. When the displacements of all Pb and halide atoms in $MAPbI_3$ and $MAPbBr_3$ are compared, the average is greater for the Br system; however, the standard deviation is greater for I.

Polaronic contributions are significant in nano systems.[14,57] Strong polaronic activity is also linked to defects and surfaces[10,11] which commonly occur in nanoscale systems. While present systems were designed to be large enough to approximate the bulk, they are in fact perhaps closer to nanosystems with a large surface-to-volume ratio and probably overestimate the polaronic contributions in terms of absolute numbers.

In summary, our DFT modeling of polaronic features compared structural distortions and energetics across several experimentally relevant halide perovskite materials. The most consistent trend identified is that electron polarons and hole polarons exhibit very different structural deformations. Across the materials studied, electron polaron formation is manifested by Jahn−Teller-like distortions in the central octahedron, with apical PbI bonds expanding about 25% and equatorial PbI bonds expanding about 2%. In contrast, hole polarons cause the central octahedron to uniformly contract by about 5%. This different structural footprint for formation of electron and hole polarons can be a tool to determine what is taking place in individual systems and devices, so that electron phonon phenomena and dynamics can be optimized accordingly. We observe that for electrons, the polaron binding energy in I-based compounds gets smaller as the A-site cation is changed from MA to Cs to FA. The local softness of the lattice in iodide compounds leads to smaller neutral reorganization energy than in bromide compounds. $MASnI_3$ has smaller polaron binding energies for electrons and holes compared to $MAPbI_3$. Finally, it is also found that the amount of change of in-plane tilt between the optimized neutral and charged structures is a good proxy for polaron binding energy. A future perspective of the present work on small polaron localization will be to study the impact of the long-range part of the interaction with the lattice on the stabilization energy.

The computational details follow ref 9. DFT calculations of HOP isolated clusters were performed using the CAM-B3LYP functional combined with the LANL2dz (for Pb, Sn, Br, Cs, and I) and 6-31G* (for N, C, and H) basis sets using *Gaussian 09* software package.[58] Because of the size of the system, use of hybrid functional, and intentional use of a local basis function, spin−orbit coupling could not be taken into account for these calculations.

■ ASSOCIATED CONTENT

Ⓢ Supporting Information

The Supporting Information is available free of charge on the ACS Publications website at DOI: 10.1021/acs.jpclett.8b03343.

Further discussion of computational details, explanation of reorganization energy definitions, and spin density comparing the electron polaron in $CsPbBr_3$ and $FAPbBr_3$ (PDF)

■ AUTHOR INFORMATION

Corresponding Author

*E-mail: ajneukirch@lanl.gov.

ORCID

Amanda J. Neukirch: 0000-0002-6583-0086
Liujiang Zhou: 0000-0001-5814-4486
Laurent Pedesseau: 0000-0001-9414-8644
Jacky Even: 0000-0002-4607-3390
Aditya D. Mohite: 0000-0001-8865-409X
Claudine Katan: 0000-0002-2017-5823
Sergei Tretiak: 0000-0001-5547-3647

Notes

The authors declare no competing financial interest.

■ ACKNOWLEDGMENTS

The work at Los Alamos National Laboratory (LANL) was supported by the LANL LDRD program (A.J.N., I.I.A., L.Z., W.N, H.T., J.J.C., and S.T.). This work was done in part at Center for Nonlinear Studies (CNLS) and the Center for Integrated Nanotechnologies CINT), a U.S. Department of Energy and Office of Basic Energy Sciences user facility, at LANL. This research used resources provided by the LANL Institutional Computing Program. Los Alamos National Laboratory is operated by Triad national Security, LLC, for the National Nuclear Security Administration of U.S. Department of Energy (Contract No. 89233218NCA000001). The work in France was supported by Agence Nationale pour la Recherche (TRANSHYPERO project). J.E. acknowledges financial support from the Institut Universitaire de France. A.D.M acknowledges the DOE-EERE 0001647-1544 grant for this work. A.J.N. thanks Mikael Kepenekian for useful insight and discussion on the setup of the calculations.

■ REFERENCES

(1) Wang, J.; Wang, N.; Jin, Y.; Si, J.; Tan, Z.; Du, H.; Cheng, L.; Dai, X.; Bai, S.; He, H.; et al. Interfacial Control Toward Efficient and Low-Voltage Perovskite Light-Emitting Diodes. *Adv. Mater.* **2015**, *27*, 2311−2316.

(2) Yuan, M.; Quan, L. N.; Comin, R.; Walters, G.; Sabatini, R.; Voznyy, O.; Hoogland, S.; Zhao, Y.; Beauregard, E. M.; Kanjanaboos, P.; et al.et al. Perovskite Energy Funnels for Efficient Light-Emitting Diodes. *Nat. Nanotechnol.* **2016**, *11*, 872.

(3) Luo, J.; Im, J.-H.; Mayer, M. T.; Schreier, M.; Nazeeruddin, M. K.; Park, N.-G.; Tilley, S. D.; Fan, H. J.; Gratzel, M. Water Photolysis at 12.3% Efficiency via Perovskite Photovoltaics and Earth-Abundant Catalysts. *Science* **2014**, *345* (6204), 1593−1596.

(4) Yakunin, S.; Sytnyk, M.; Kriegner, D.; Shrestha, S.; Richter, M.; Matt, G. J.; Azimi, H.; Brabec, C. J.; Stangl, J.; Kovalenko, M. V.; et al. Detection of X-Ray Photons by Solution-Processed Lead Halide Perovskites. *Nat. Photonics* **2015**, *9* (7), 444−U44.

(5) Yakunin, S.; Dirin, D. N.; Shynkarenko, Y.; Morad, V.; Cherniukh, I.; Nazarenko, O.; Kreil, D.; Nauser, T.; Kovalenko, M. Detection of Gamma Photons Using Solution-Grown Single Crystals of Hybrid Lead Halide Perovskites. *Nat. Photonics* **2016**, *10*, 585−589.

(6) Kepenekian, M.; Robles, R.; Katan, C.; Sapori, D.; Pedesseau, L.; Even, J. Rashba and Dresselhaus Effects in Hybrid Organic-Inorganic Perovskites: From Basics to Devices. *ACS Nano* **2015**, *9* (12), 11557−11567.

(7) Muthu, C.; Nagamma, S. R.; Nair, V. C. Luminescent Hybrid Perovskite Nanoparticles as a New Platform for Selective Detection of 2,4,6-Trinitrophenol. *RSC Adv.* **2014**, *4* (99), 55908−55911.

(8) Nie, W.; Blancon, J.; Neukirch, A. J.; Appavoo, K.; Tsai, H.; Chhowalla, M.; Alam, M. A.; Sfeir, M. Y.; Katan, C.; Even, J.; et al. Light-Activated Photocurrent Degradation and Self-Healing in Perovskite Solar Cells. *Nat. Commun.* **2016**, *7*, 11574.

(9) Neukirch, A. J.; Nie, W.; Blancon, J.-C.; Appavoo, K.; Tsai, H.; Sfeir, M. Y.; Katan, C.; Even, J.; Crochet, J. J.; Gupta, G.; et al. Polaron Stabilization by Cooperative Lattice and Cation Rotations in Hybrid Perovskite Materials. *Nano Lett.* **2016**, *16* (6), 3809−3816.

(10) Diab, H.; Trippé-Allard, G.; Lédée, F.; Jemli, K.; Vilar, C.; Bouchez, G.; Jacques, V. L. R.; Tejeda, A.; Even, J.; Lauret, J. S.; et al. Narrow Linewidth Excitonic Emission in Organic-Inorganic Lead Iodide Perovskite Single Crystals. *J. Phys. Chem. Lett.* **2016**, *7* (24), 5093−5100.

(11) Ivanovska, T.; Dionigi, C.; Mosconi, E.; De Angelis, F.; Liscio, F.; et al. Long-Lived Photoinduced Polarons in Organohalide Perovskites. *J. Phys. Chem. Lett.* **2017**, *8*, 3081−3086.

(12) Park, M.; Neukirch, A. J.; Reyes-Lillo, S. E.; Lai, M.; Ellis, S. R.; Dietze, D.; Neaton, J. B.; Yang, P.; Tretiak, S.; Mathies, R. A. Excited-State Vibrational Dynamics toward the Polaron in Methylammonium Lead Iodide Perovskite. *Nat. Commun.* **2018**, *9* (1), 2525.

(13) Wei, T.-C.; Wang, H.-P.; Li, T.-Y.; Lin, C.-H.; Hsieh, Y.-H.; Chu, Y.-H.; He, J.-H. Photostriction of $CH_3NH_3PbBr_3$ Perovskite Crystals. *Adv. Mater.* **2017**, *29* (35), 1701789.

(14) Zheng, K.; Abdellah, M.; Zhu, Q.; Kong, Q.; Jennings, G.; Kurtz, C. A.; Messing, M. E.; Niu, Y.; Gosztola, D. J.; Al-marri, M. J.; et al. Direct Experimental Evidence for Photoinduced Strong-Coupling Polarons in Organolead Halide Perovskite Nanoparticles. *J. Phys. Chem. Lett.* **2016**, *7*, 4535−4539.

(15) Bischak, C. G.; Hetherington, C. L.; Wu, H.; Aloni, S.; Ogletree, D. F.; Limmer, D. T.; Ginsberg, N. S. Origin of Reversible Photoinduced Phase Separation in Hybrid Perovskites. *Nano Lett.* **2017**, *17*, 1028−1033.

(16) Santomauro, F. G.; Grilj, J.; Mewes, L.; Nedelcu, G.; Yakunin, S.; Rossi, T.; Haddad, A. Al; Budarz, J.; Kinschel, D.; Ferreira, D. S.; et al. Localized Holes and Delocalized Electrons in Photoexcited Inorganic Perovskites: Watching Each Atomic Actor by Picosecond X-Ray Absorption Spectroscopy. *Struct. Dyn.* **2017**, *4*, No. 044002.

(17) Yin, J.; Li, H.; Cortecchia, D.; Soci, C.; Bredas, J. Excitonic and Polaronic Properties of 2D Hybrid Organic − Inorganic Perovskites. *ACS Energy Lett.* **2017**, *2*, 417−423.

(18) Cortecchia, D.; Bruno, A.; Lo, S.-Z. A.; Gurzadyan, G. G.; Mhaisalkar, S.; Bredas, J.-L.; Soci, C. Polaron Self-Localization in White-Light Emitting Hybrid Perovskites. *J. Mater. Chem. C* **2017**, *5* (11), 2771−2780.

(19) Mccall, K. M.; Stoumpos, C. C.; Kostina, S. S.; Kanatzidis, M. G.; Wessels, B. W. Strong Electron − Phonon Coupling and Self-Trapped Excitons in the Defect Halide Perovskites $A_3M_2I_9$ (A = Cs, Rb ; M = Bi, Sb). *Chem. Mater.* **2017**, *29* (9), 4129−4145.

(20) Nilă, A.; Baibarac, M.; Matea, A.; Mitran, R.; Baltog, I. Exciton−phonon Interactions in the Cs3Bi2I9 Crystal Structure Revealed by Raman Spectroscopic Studies. *Phys. Status Solidi B* **2017**, *254* (4), 1552805.

(21) Kim, G. Y.; Senocrate, A.; Yang, T.; Gregori, G.; Grätzel, M.; Maier, J. Large Tunable Photoeffect on Ion Conduction in Halide Perovskites and Implications for Photodecomposition. *Nat. Mater.* **2018**, *17* (May), 445−450.

(22) Yamada, K.; Nishikubo, R.; Oga, H.; Ogomi, Y.; Hayase, S.; Kanno, S.; Imamura, Y.; Hada, M.; Saeki, A. Anomalous Dielectric Behavior of a Pb/Sn Perovskite: Effect of Trapped Charges on Complex Photoconductivity. *ACS Photonics* **2018**, *5*, 3189.

(23) Obraztsov, P. A.; Lyashenko, D.; Chizhov, P. A.; Konishi, K.; Nemoto, N.; Kuwata-gonokami, M.; Welch, E.; Obraztsov, A. N.; Zakhidov, A. Ultrafast Zero-Bias Photocurrent and Terahertz Emission in Hybrid Perovskites. *Commun. Phys.* **2018**, *1*, 14.

(24) Katan, C.; Pedesseau, L.; Kepenekian, M.; Rolland, A.; Even, J. Interplay of Spin-Orbit Coupling and Lattice Distortion in Metal Substituted 3D Tri-Chloride Hybrid Perovskites. *J. Mater. Chem. A* **2015**, *3* (17), 9232−9240.

(25) Welch, E.; Scolfaro, L.; Zakhidov, A. Density Functional Theory + U Modeling of Polarons in Organohalide Lead Perovskites Density Functional Theory + U Modeling of Polarons in Organohalide Lead Perovskites. *AIP Adv.* **2016**, *6*, 125037.

(26) Jishi, R. A.; Ta, O. B.; Sharif, A. A. Modeling of Lead Halide Perovskites for Photovoltaic Applications. *J. Phys. Chem. C* **2014**, *118*, 28344−28349.

(27) NREL. Best Research-cell Efficiencies.

(28) Baikie, T.; Fang, Y.; Kadro, J. M.; Schreyer, M.; Wei, F.; Mhaisalkar, S. G.; Gratzel, M.; White, T. J. Synthesis and Crystal Chemistry of the Hybrid Perovskite $(CH_3NH_3)PbI_3$ for Solid-State Sensitised Solar Cell Applications. *J. Mater. Chem. A* **2013**, *1* (18), 5628.

(29) Trots, D. M.; Myagkota, S. V. High-Temperature Structural Evolution of Caesium and Rubidium Triiodoplumbates. *J. Phys. Chem. Solids* **2008**, *69* (10), 2520−2526.

(30) Wang, P.; Guan, J.; Galeschuk, D. T. K.; Yao, Y.; He, C. F.; Jiang, S.; Zhang, S.; Liu, Y.; Jin, M.; Jin, C.; et al. Pressure-Induced Polymorphic, Optical, and Electronic Transitions of Formamidinium Lead Iodide Perovskite. *J. Phys. Chem. Lett.* **2017**, *8* (10), 2119−2125.

(31) Brivio, F.; Caetano, C.; Walsh, A. Thermodynamic Origin of Photoinstability in the $CH_3NH_3Pb(I_{1-x}Br_x)_3$ Hybrid Halide Perovskite Alloy. *J. Phys. Chem. Lett.* **2016**, *7* (6), 1083−1087.

(32) Hoke, E. T.; Slotcavage, D. J.; Dohner, E. R.; Bowring, A. R.; Karunadasa, H. I.; McGehee, M. D. Reversible Photo-Induced Trap Formation in Mixed-Halide Hybrid Perovskites for Photovoltaics. *Chem. Sci.* **2015**, *6* (1), 613−617.

(33) Draguta, S.; Sharia, O.; Yoon, S. J.; Brennan, M. C.; Morozov, Y. V.; Manser, J. M.; Kamat, P. V.; Schneider, W. F.; Kuno, M. Rationalizing the Light-Induced Phase Separation of Mixed Halide Organic−inorganic Perovskites. *Nat. Commun.* **2017**, *8* (1), 200.

(34) Soufiani, A. M.; Huang, F.; Reece, P.; Sheng, R.; Ho-Baillie, A.; Green, M. A. Polaronic Exciton Binding Energy in Iodide and Bromide Organic-Inorganic Lead Halide Perovskites. *Appl. Phys. Lett.* **2015**, *107* (23), 231902.

(35) Swainson, I. P.; Hammond, R. P.; Soullière, C.; Knop, O.; Massa, W. Phase Transitions in the Perovskite Methylammonium Lead Bromide, $CH_3ND_3PbBr_3$. *J. Solid State Chem.* **2003**, *176* (1), 97−104.

(36) Swainson, I. P.; Tucker, M. G.; Wilson, D. J.; Winkler, B.; Milman, V. Pressure Response of an Organic-Inorganic Perovskite: Methylammonium Lead Bromide. *Chem. Mater.* **2007**, *19* (10), 2401−2405.

(37) Stoumpos, C. C.; Malliakas, C. D.; Peters, J. A.; Liu, Z.; Sebastian, M.; Im, J.; Chasapis, T. C.; Wibowo, A. C.; Chung, D. Y.; Freeman, A. J.; et al. Crystal Growth of the Perovskite Semiconductor $CsPbBr_3$: A New Material for High-Energy Radiation Detection. *Cryst. Growth Des.* **2013**, *13* (7), 2722−2727.

(38) Stoumpos, C. C.; Malliakas, C. D.; Kanatzidis, M. G. Semiconducting Tin and Lead Iodide Perovskites with Organic Cations: Phase Transitions, High Mobilities, and near-Infrared Photoluminescent Properties. *Inorg. Chem.* **2013**, *52* (15), 9019−9038.

(39) Zuppiroli, L.; Bieber, A.; Michoud, D.; Galli, G.; Gygi, F.; Bussac, M.; Andre, J. Polaron Formation and Symmetry Breaking. *Chem. Phys. Lett.* **2003**, *374*, 7−12.

(40) Holstein, T. Studis of Polaron Motion: Part II. The "Small" Polaron. *Ann. Phys. (Amsterdam, Neth.)* **1959**, *389*, 343−389.

(41) Goodenough, J. B. JAHN-TELLER PHENOMENA IN SOLIDS. *Annu. Rev. Mater. Sci.* **1998**, *28*, 1−27.

(42) Koppel, H.; Yarkony, D.; Barentzen, H. *The Jahn-Teller Effect*; Springer: Heidelberg, 2009.

(43) Varignon, J.; Bristowe, N. C.; Ghosez, P. Electric Field Control of Jahn-Teller Distortions in Bulk Perovskites. *Phys. Rev. Lett.* **2016**, *116*, 057602.

(44) Lee, J.; Lee, H.; Averitt, R.; Trugman, S.; Demsar, J.; Funk, D.; Hur, N.; Moritomo, Y.; Taylor, A. J.; Prasankumar, R. P.; et al. Ultrafast Polaron Dynamics in Layered and Perovskite Manganites: 2D and 3D Polarons. 2016, arXiv:1609.09155.

(45) Kepenekian, M.; Traore, B.; Blancon, J.-C.; Pedesseau, L.; Tsai, H.; Nie, W.; Stoumpos, C. C.; Kanatzidis, M. G.; Even, J.; Mohite, A. D.; et al. Concept of Lattice Mismatch and Emergence of Surface States in Two-Dimensional Hybrid Perovskite Quantum Wells¨. *Nano Lett.* **2018**, *18* (9), 5603−5609.

(46) Knutson, J. L.; Martin, J. D.; Mitzi, D. B. Tuning the Band Gap in Hybrid Tin Iodide Perovskite Semiconductors Using Structural Templating. *Inorg. Chem.* **2005**, *44* (13), 4699−4705.

(47) Filip, M. R.; Eperon, G. E.; Snaith, H. J.; Giustino, F. Steric Engineering of Metal-Halide Perovskites with Tunable Optical Band Gaps. *Nat. Commun.* **2014**, *5*, 5757.

(48) Pedesseau, L.; Sapori, D.; Traore, B.; Robles, R.; Fang, H.-H.; Loi, M. A.; Tsai, H.; Nie, W.; Blancon, J.-C.; Neukirch, A.; et al.

Advances and Promises of Layered Halide Hybrid Perovskite Semiconductors. *ACS Nano* **2016**, *10* (11), 9776−9786.

(49) Traore, B.; Pedesseau, L.; Assam, L.; Che, X.; Blancon, J. C.; Tsai, H.; Nie, W.; Stoumpos, C. C.; Kanatzidis, M. G.; Tretiak, S.; et al. Composite Nature of Layered Hybrid Perovskites: Assessment on Quantum and Dielectric Confinements and Band Alignment. *ACS Nano* **2018**, *12* (4), 3321−3332.

(50) Bao, Z.; Locklin, J. *Organic Field-Effect Transistors*; CRC Press: Boca Raton, FL, 2007.

(51) Marcus, R. A. Electron Transfer Reactions in Chemistry: Theory and Experiment (Nobel Lecture). *Angew. Chem., Int. Ed. Engl.* **1993**, *32* (8), 1111−1121.

(52) Ferreira, A. C.; Létoublon, A.; Paofai, S.; Raymond, S.; Ecolivet, C.; Rufflé, B.; Cordier, S.; Katan, C.; Saidaminov, M. I.; Zhumekenov, A. A.; et al. Elastic Softness of Hybrid Lead Halide Perovskites. *Phys. Rev. Lett.* **2018**, *121*, 085502.

(53) Wright, A. D.; Verdi, C.; Milot, R. L.; Eperon, G. E.; Pérez-Osorio, M. A.; Snaith, H. J.; Giustino, F.; Johnston, M. B.; Herz, L. M. Electron-Phonon Coupling in Hybrid Lead Halide Perovskites. *Nat. Commun.* **2016**, *7*, 11755.

(54) Zhu, X. Y.; Podzorov, V. Charge Carriers in Hybrid Organic-Inorganic Lead Halide Perovskites Might Be Protected as Large Polarons. *J. Phys. Chem. Lett.* **2015**, *6* (23), 4758−4761.

(55) Katan, C.; Mohite, A. D.; Even, J. Entropy in Halide Perovskites. *Nat. Mater.* **2018**, *17* (5), 377−379.

(56) Murtaza, G.; Ahmad, I. First Principle Study of the Structural and Optoelectronic Properties of Cubic Perovskites $CsPbM_3$(M = Cl, Br, I). *Phys. B* **2011**, *406* (17), 3222−3229.

(57) Telfah, H.; Jamhawi, A.; Teunis, M. B.; Sardar, R.; Liu, J. Ultrafast Exciton Dynamics in Shape-Controlled Methylammonium Lead Bromide Perovskite Nanostructures: Effect of Quantum Confinement on Charge Carrier Recombination. *J. Phys. Chem. C* **2017**, *121* (51), 28556−28565.

(58) Frisch, M. J.; Trucks, G. W.; Schlegel, H. B.; Scuseria, G. E.; Robb, M. A.; Cheeseman, J. R.; Scalmani, G.; Barone, V.; Mennucci, B.; Petersson, G. A.; et al. *Gaussian09*, revision A.1; Gaussian Inc.: Wallingford, CT, 2009.